Curvelet-domain multiple elimination with sparsness constraints

SLIM
Seismic Laboratory for Imaging and Modeling

Felix J. Herrmann [1] (fherrmann@eos.ubc.ca) and Dirk J. (Eric) Verschuur [2] (d.j.verschuur@tnw.tudelft.nl)
[1] Department of Earth and Ocean Sciences - University of British Columbia, Canada
[2] Faculty of Applied Sciences - Delft University of Technology, The Netherlands

Summary

A non-linear primary-multiple separation method using curvelet frames is presented. The near optimal representation by 2-D/3-D curvelet frames of primaries and multiples leads to a primary-multiple separation scheme that:

- is robust under the presence of noise and missing data
- represents both signal components with a limited number of multi-scale and directional atoms
- separates on the basis of differences in locations, orientation, and scale of the two components
- minimizes correlations between the coefficients of the two components

We compare our results with conventional adaptive subtraction techniques based on (windowed) matched filtering.

Field data example, Gulf of Mexico

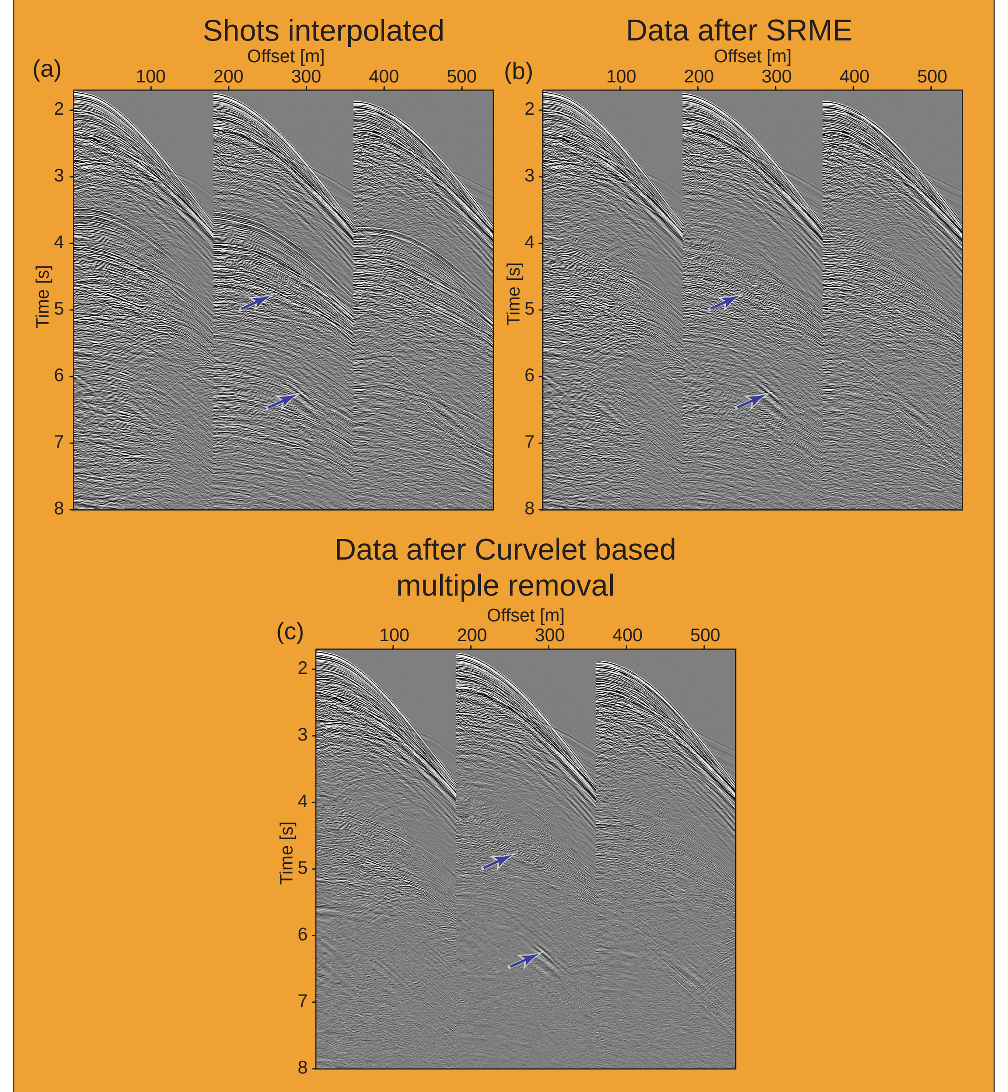

Figure 1: Comparison between the conventional surface-related multiple elimination (SRME) (b) and the curvelet subtraction based on an iterative blocksolver (c) . The dataset containing the primaries and multiples is given in (a).

Characteristics of Curvelets

Curvelets are:

- Nonseperable
- Localized in the Space and Fourier domain
- Anisotropic ($\mathrm{length}^2 \approx \mathrm{width}$)
- Multiscale
- Optimal tight frame
- Near orthogonal

Curvelet resolution

Second dyadic partitioning

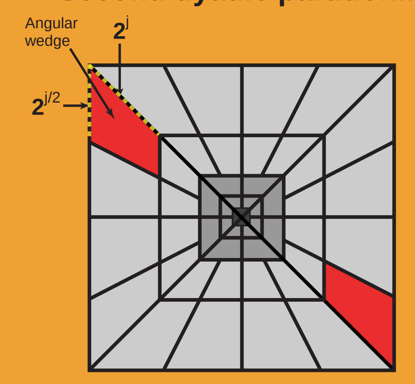

Figure 2: Description of the second dyadic partitioning for curvelets at different scales and orientations.

Partitioning example

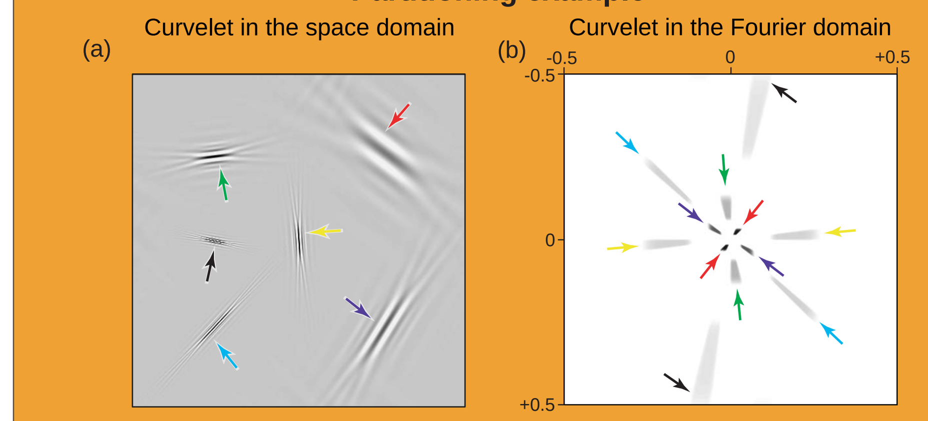

Figure 3: Example using six different curvelets, representing the localization property of curvelets in both space (a) and frequency (b).

Why we use curvelets for signal separation

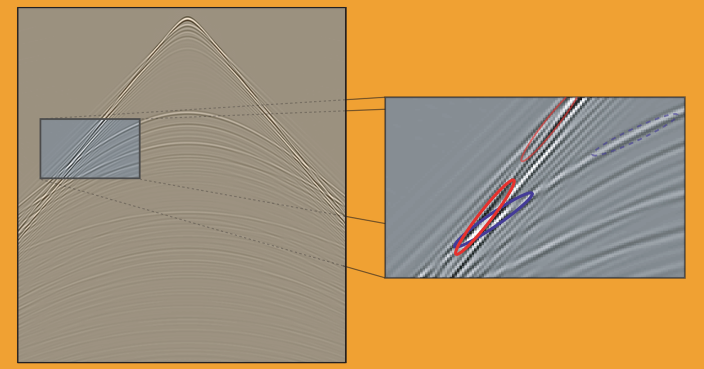

Figure 4: Description of the signal separation using curvelet frame. Although the two signals interfere, they will be they will be clearly separated in the curvelet domain based on angular wedge where their significant contributions will be located.

Signal separation approach

Our method is based on the separation of the data into the primary $\mathbf{s}_1$ and multiple $\mathbf{s}_2$ component in the presence of white gaussian noise $\mathbf{n}$,

$$\mathbf{s} = \mathbf{s_1} + \mathbf{s_2} + \mathbf{n}.$$

This separation problem was solved using the following minimization,

$$\hat{\mathbf{s}} = \arg\min_c \frac{1}{2}||\mathbf{s} - \mathbf{Tc}||_2^2 + ||\mathbf{c}||_{p,w}$$

whereas

$$\mathbf{T} = [\mathbf{T_1} \quad \mathbf{T_2}],\ \mathbf{c} = [\mathbf{c_1} \quad \mathbf{c_2}]^T, \text{ and } \mathbf{w} = [\mathbf{w_1} \quad \mathbf{w_2}]^T.$$

$\mathbf{T}_1, \mathbf{T}_2$: Frame composition of the primaries ($\mathbf{T}_1$) and multiples ($\mathbf{T}_2$)
$\mathbf{c}$: Frame coefficient vector
$||\mathbf{c}||_{p,w}$: p-Norm of the coefficients weighted by the vector $w_i > 0$, whereas $1 \leq p < 2$
$\mathbf{w}_1(\lambda) = \lambda|\check{\mathbf{c}}_2|, \mathbf{w}_2(\lambda) = \lambda|\check{\mathbf{c}}_1|$: Weighting of the predicted two components

Curvelets in 3-D

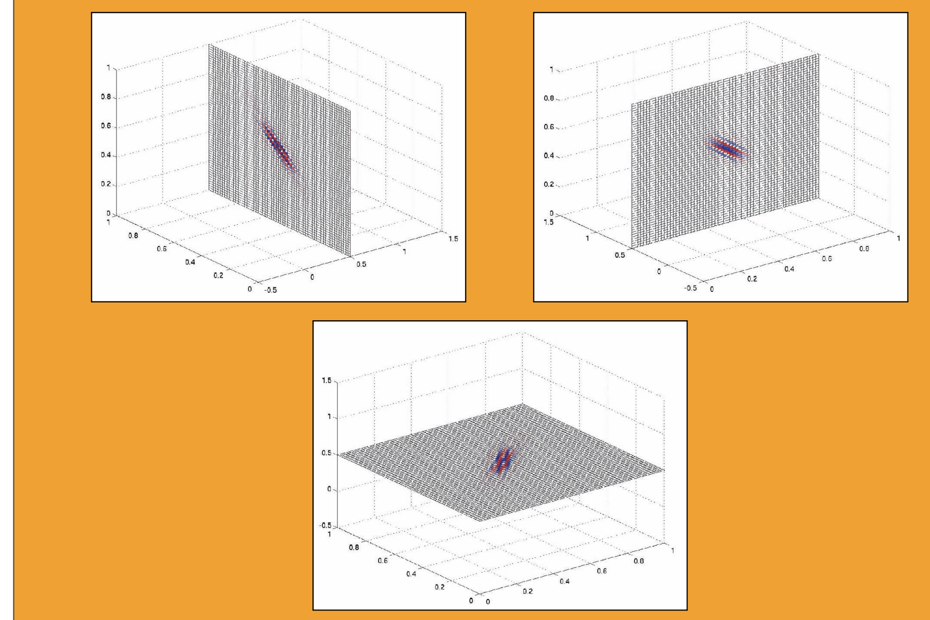

Figure 5: The three faces of a 3-D Curvelet. Courtesy [CurveLab 3]

Explanation of soft thresholding

$$S_w^s = \begin{cases} x - w & \text{if} \quad x \geq w \\ x + w & \text{if} \quad x \leq -w \\ 0 & \text{if} \quad |x| < w \end{cases}$$

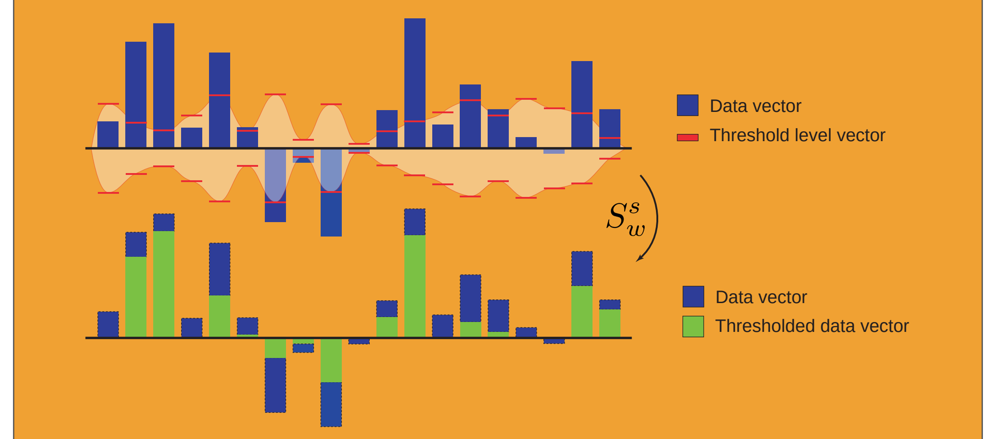

Figure 6: Application of a threshold level vector on an arbitrary data vector, resulting in a thresholded data vector.

Description of the iterative blocksolver algorithm used to solve the minimization problem

1. Initialize L_{max}, number of iterations
2. Calculate $c^{tot} = T^*(s) = \left[c_1^{tot} \quad c_2^{tot}\right]^T$
3. Perform L_{max} times

   Part A
   - Update $\mathbf{c}_2$ assuming $\mathbf{c}_1$ is fixed
   - Set $\delta_1 = \mathbf{w}_2(\lambda) \cdot L_{max}$
   - Calculate the residual $\mathbf{R} = \mathbf{s} - \mathbf{T}_1\mathbf{c}_1 - \mathbf{T}_2\mathbf{c}_2$
   - Calculate $\boldsymbol{\alpha}_1 = \mathbf{c}_1 + \mathbf{T}_1^*(\mathbf{R})$
   - Calculate $\hat{\boldsymbol{\alpha}}_1 = S_{\delta_1}^s(\boldsymbol{\alpha}_1)$
   - Reconstruct $\tilde{\mathbf{c}}_2 = c_2^{tot} - \hat{\boldsymbol{\alpha}}_1$
   - Update $\delta_1 = \delta_1 - \mathbf{w}_2(\lambda)$

   Part B
   - Update $\mathbf{c}_1$ assuming $\mathbf{c}_2$ is fixed
   - Set $\delta_2 = \mathbf{w}_1(\lambda) \cdot L_{max}$
   - Calculate the residual $\mathbf{R} = \mathbf{s} - \mathbf{T}_1\mathbf{c}_1 - \mathbf{T}_2\mathbf{c}_2$
   - Calculate $\boldsymbol{\alpha}_2 = \mathbf{c}_2 + \mathbf{T}_2^*(\mathbf{R})$
   - Calculate $\hat{\boldsymbol{\alpha}}_2 = S_{\delta_2}^s(\boldsymbol{\alpha}_2)$
   - Reconstruct $\tilde{\mathbf{c}}_1 = c_1^{tot} - \hat{\boldsymbol{\alpha}}_2$
   - Update $\delta_2 = \delta_2 - \mathbf{w}_1(\lambda)$
4. End

Correlation between the primaries and multiples using three different bases

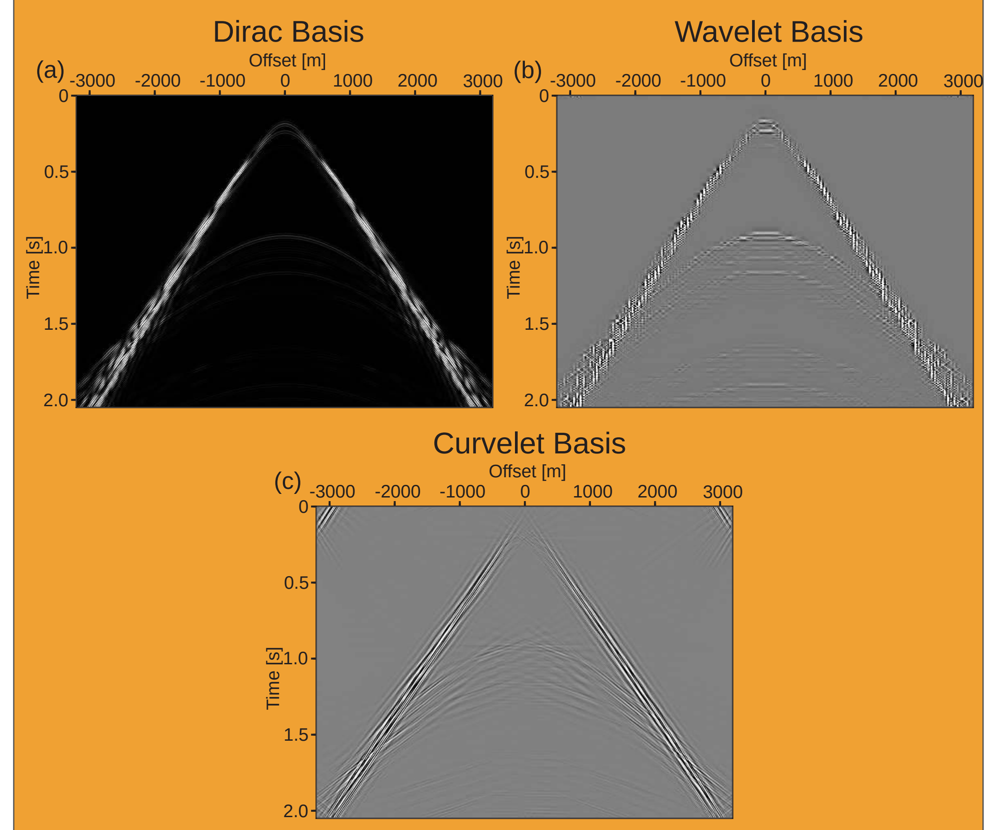

Figure 7: Correlations between the coefficients of the primaries and multiples are computed by multiplying the coefficients, for the Dirac (a), the Wavelet (b), and the Curvelet (c) basis, followed by an inverse transform. Curvelets potentially separate the best, because they are the least correlated

2-D Synthetic Example

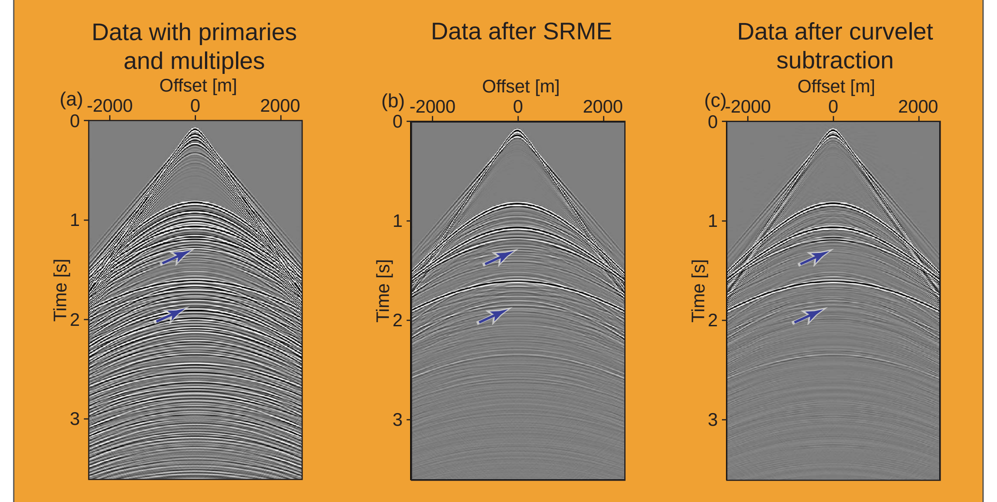

Figure 8: Predicted primaries for a synthetic dataset (a) using the matched-filter method (b) and the curvelet approach (c). Clearly, the curvelets (c) produce a better separation result.

3-D Synthetic Dataset

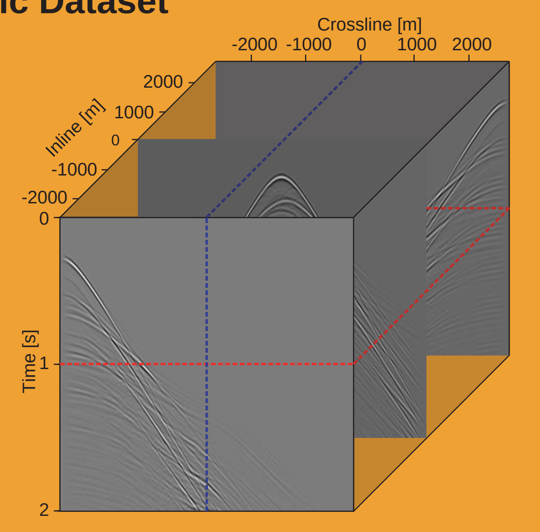

Figure 9: Synthetic 3-D dataset used for the comparisons made in figure 10 and 11. The dimensions of the presented dataset are 361 x 361 x 501. The red (t = 1 s) and blue (Crossline = 0 m) line correspond to the location of the slices on the right.

3-D Synthetic Example

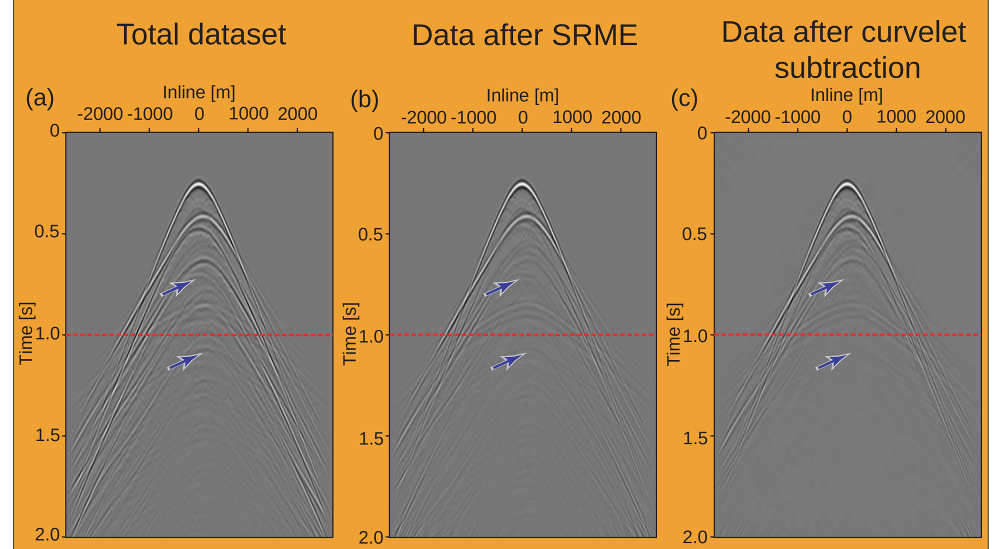

Figure 10: Section of the input (a) dataset containing the primaries and multiples, the SRME result, and the curvelet subtraction taken at 0 m crossline. The blue arrows indicate areas of major interest.

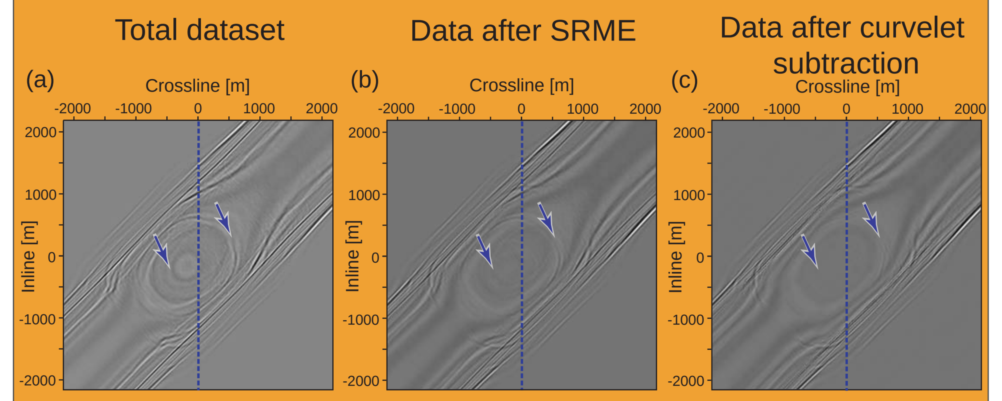

Figure 11: Time slices (taken at 1 s) of the input dataset (a), the SRME subtraction result (b), and the curvelet subtraction result (c). Clearly, curvelet subtraction outperforms the conventional SRME subtraction approach, highlighted by blue arrows.

Total dataset - predicted primaries

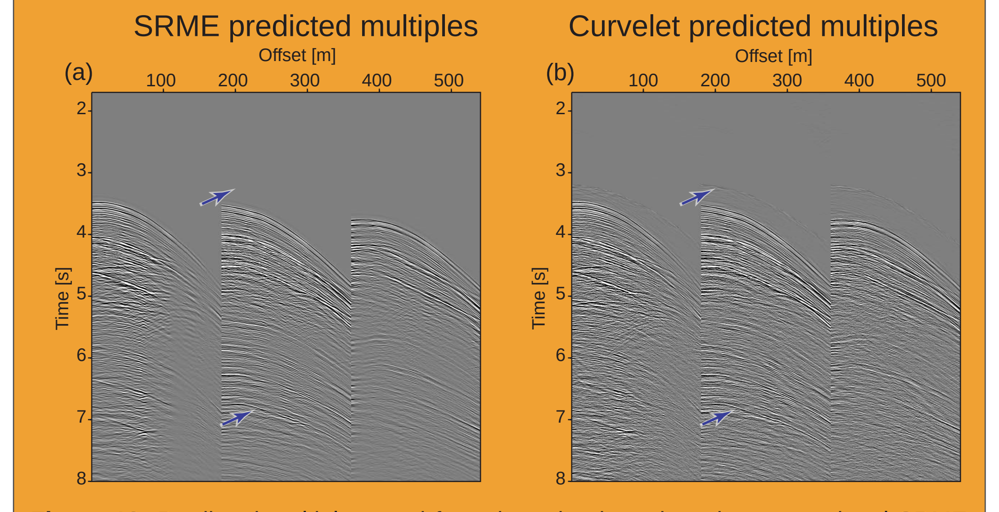

Figure 12: Predicted multiples used for subtraction based on the conventional SRME (a) approach and the curvelet (b) method. Blue arrows indicate areas of major interest.

3-D field dataset

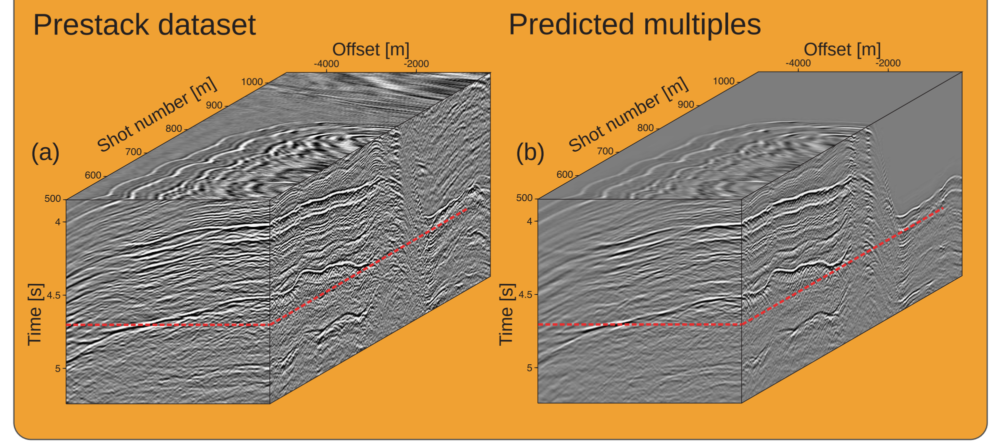

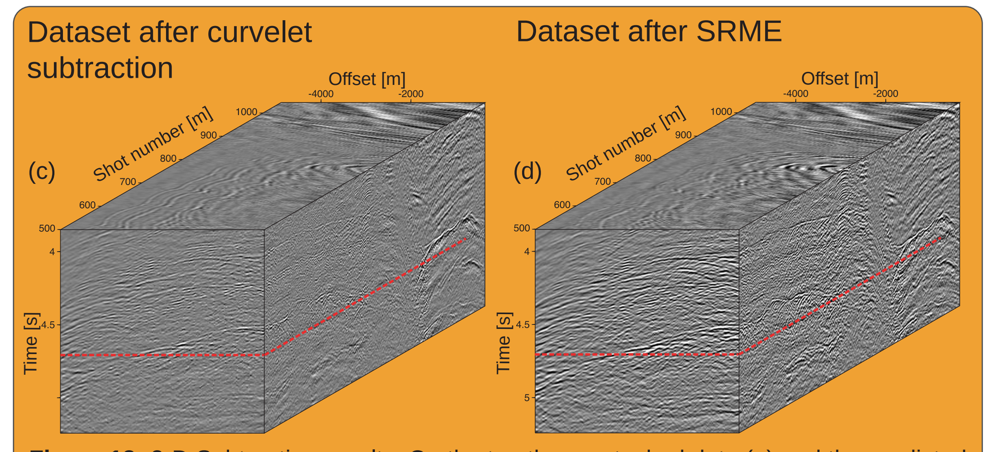

Figure 13: 3-D Subtraction results. On the top the prestacked data (a) and the predicted multiples (b) are given. (c) and (d) correspond to the curvelet and SRME subtraction results. The red line correponds to the position of the time slices shown below.

2-D Time slices

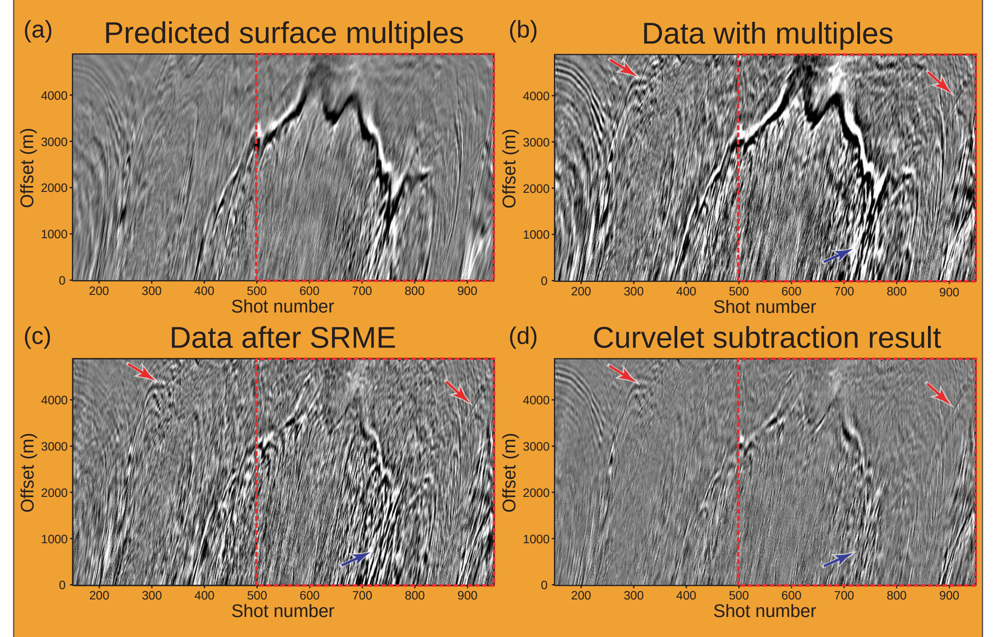

Figure 14: 3-D Subtraction results at t = 4.7 s. Red arrows indicate primary events, blue arrows indicate an area with a clearly better subtraction result using the curvelet frame compared to the conventional SRME.

Discussion and Conclusions

The success of our approach essentially derives from the parsimoniousness of curvelet frames with respect to seismic data. As such, simple (iteratative) soft thresholding procedures on the coefficients, based on weights that depend on the magnitude of the coefficients only, suffice to effectively separate primaries from multiples. Soft thresholding can be seen as a mask that mutes those regions in the data that with high probability pertain the other signal component. The method derives its robustness from:

- the sparsness of the primary and multiple curvelet vectors
- the unlikelyness that large entries in the curvelet vector over lap
- the robustness on real datasets and the improvement over adaptive subtraction with matched filtering

Acknowledgments

The author would like to thank the authors of CurveLab: Fast Discrete Curvelet transform. We would like to thank Urs Boeniger for making this poster, J. F. Paradis, M. Beyreuther and G. Hennenfent for helping with coding. This work was carried out as part of the SINBAD project with financial support, secured through ITF (the Industry Technology Facilitator), from the following organizations: BG Group, BP, ExxonMobil and SHELL. The authors also thank Western Geco for providing the field dataset. Additional funding came from the NSERC Discovery Grant 22R81254.